Materials Advances

ROYAL SOCIETY OF CHEMISTRY

PAPER

View Article Online
View Journal

Check for updates

Cite this: DOI: 10.1039/d5ma01298h

Upcycling *Sargassum* biomass into biodegradable mulch films *via* sodium alginate and recycled polyvinyl alcohol

Aldair Etmar Garcia,[a] Mengyao Gao, *[a] Jing-Xian Chen,[a] Ying Wang*[b] and Seth W. Snyder[c]

Sargassum accumulations along tropical coastlines create major environmental and socioeconomic burdens due to odor, ecosystem disruption, and high cleanup costs. Here, we develop biodegradable mulch films that valorize *Sargassum*-derived sodium alginate (SA) blended with recycled polyvinyl alcohol (PVA), glycerol (plasticizer), and zein (functional additive), followed by beeswax surface coating to improve water resistance. The coated films achieved tunable hydrophobicity (water contact angle 73.6–116.5°) and tensile strength of ≥8 MPa (up to ~13 MPa without coating), with strong UV shielding (<1% transmittance below 400 nm). Under outdoor rainfall and sunlight exposure, double-side coated films fully degraded within 35 days. Soil safety was supported by OECD Guideline 207 testing with *Eisenia fetida*, showing 0% mortality. These results demonstrate a low-toxicity pathway to convert *Sargassum* waste and recycled polymer into functional biodegradable mulch films for agricultural applications.

Received 10th November 2025,
Accepted 8th April 2026

DOI: 10.1039/d5ma01298h

rsc.li/materials-advances

Open Access Article. Published on 11 May 2026. Downloaded on 6/2/2026 12:52:24 PM.
This article is licensed under a Creative Commons Attribution-NonCommercial 3.0 Unported Licence.

1. Introduction

Managing biomass waste: omass degradation and soil processes are now recognized as major sources of greenhouse gas (GHG) emissions, releasing not only carbon dioxide (CO_2) but also more potent gases such as methane (CH_4) and nitrous oxide (N_2O), largely driven by anthropogenic activities.[1] Despite ongoing global efforts, there is still a lack of comprehensive research and knowledge to achieve net-zero emissions. Modak *et al.*[2] state that the projected CO_2 emissions for the year 2030 will primarily result from the burning of fossil fuels, including coal, natural gas, and oil, for energy and transportation. Although a significant proportion of GHG emissions originates from industrial activities and changes in land use, the main emission is CO_2, which was approximately 37 billion metric tons in 2023.[3–5]

Collecting waste products and converting them into valuable biodegradable mulch films offers a sustainable approach to improving agricultural practices. The *Sargassum* from the great atlantic *Sargassum* belt (GASB) that is washed up to the shore becomes waste, potentially contributing to air pollution due to the strong odor that may be unpleasant for the tourism industry.[6] Thus, research must be done to convert this waste into value-added material, leading to a greener world. While there is a strong interest in the Atlantic-Caribbean region to establish profitable ventures that utilize *Sargassum*, advancements have been sluggish, and there are only a limited number of instances where sustainable businesses have successfully created end products from *Sargassum*.[7–9]

The need for polymeric films: polymeric films hold significant value in numerous industrial sectors, including automotive, aerospace, electrical and electronic, chemical, and optical industries.[10,11] Additionally, these films find applications in the military, building construction, landscaping, and packaging, highlighting their widespread utility.[12,13] Thus, humans tend to use polymeric films in their daily lives. Conventional packaging materials have been transformed by incorporating petroleum-based polymers owing to their cost-effectiveness, favorable barrier properties, and robust mechanical attributes.[14] Nevertheless, the use of such packaging materials poses significant environmental challenges as they do not readily degrade in existing landfill processes, as highlighted in the literature.[15] Agricultural mulch film is generally a thin plastic film used to cover raised beds where vegetation grows, which improves crop yield by suppressing weed growth while regulating soil temperature and moisture content.[16–19]

In agriculture, mulch films are used to protect crops against pests and modify abiotic factors to attain higher crop yields.

[a] *Department of Chemical Engineering, National Taiwan University of Science and Technology, Taipei 10607, Taiwan. E-mail: mygao@mail.ntust.edu.tw*
[b] *Center for General Education, National Taiwan University of Science and Technology, Taipei 10607, Taiwan. E-mail: wannie@mail.ntust.edu.tw*
[c] *S.W. Scientific Investments LLC, Memphis, Tennessee 38120, USA*

© 2026 The Author(s). Published by the Royal Society of Chemistry

Open Access Article. Published on 11 May 2026. Downloaded on 6/2/2026 12:52:24 PM.
This article is licensed under a Creative Commons Attribution-NonCommercial 3.0 Unported Licence.

In China, the prolonged use of plastic film mulches has led to the accumulation of an estimated 50–260 kg hm^{-2} of residual plastics in the topsoil (0–20 cm), creating a risk of both environmental damage to the soil and health risk in the crop. This accumulation has the potential to hinder plant growth.[31] Creating valuable biopolymeric mulch films as a substitute for plastic films for the agriculture industry may not only lessen the toxicity of soil but also lead to a circular economy, enabling the agriculture sector to achieve net-zero emissions.[32,33] The utilization of agro-industrial and marine wastes and by-products for the production of biopolymers is regarded as a promising alternative to synthetic materials. This approach holds potential for the development of biodegradable food packages and biomaterials, presenting a sustainable option in this context.[34]

Traditional plastic mulch films are increasingly being replaced with biodegradable alternatives to prevent the accumulation of plastic residue in the soil, which contributes to plastic pollution. Biodegradable mulch films decompose rapidly, but only under controlled conditions that are often difficult to achieve in natural environments, potentially generating biodegradable microplastics. However, limited research is available to comprehend their environmental impacts fully.[35] Additionally, biodegradable mulch films face challenges such as incomplete degradation, insufficient tensile strength for mechanized application, high production costs, and environmental factors like soil conditions that affect their effectiveness, while their limitations include potential harm to soil from degradation products and reduced durability compared to traditional plastic mulch films.[36,37] If the molecular chains of sodium alginate demonstrate compatibility to form strong bonds with recycled PVA, this combination could yield a sustainable mulch film that enhances soil health by increasing carbon content over time through the gradual deposition of organic matter.[38]

Despite rapid growth in biodegradable mulch technologies, several barriers still limit real-world adoption: (i) insufficient tensile strength and tear resistance for mechanized laying and retrieval, (ii) moisture sensitivity and loss of integrity under rain-wetting/drying cycles, (iii) incomplete or slow biodegradation under variable soils and climates, and (iv) cost and scale-up challenges relative to polyethylene (PE). At the same time, opportunities are expanding through improved polymer blending, barrier coatings, and waste-derived feedstocks that support circular economy routes and reduce microplastic accumulation. Recent studies ($\leq$3 years) report progress in alginate- and PVA-based biodegradable films through stronger intermolecular networks, optimized plasticizers, and hydrophobic surface modification to enhance field durability while maintaining biodegradability. However, there remains a need for systems that simultaneously demonstrate (a) practical hydrophobicity under rainfall exposure, (b) adequate mechanical performance, and (c) verified soil safety using standardized ecotoxicity protocols.

Sargassum biomass: the natural process begins with the capture of CO_2 through photosynthesis by the macro-algae *Sargassum*, as shown in Fig. 1, found in the Sargasso Sea, which captures approximately 7% of the global net carbon emissions annually.[20] When *Sargassum* dies, it is either deposited on the ocean floor or washed onto the seashore. Sodium alginate can be extracted from *Sargassum* and utilized as a foundational building block or structural pillar for creating biodegradable mulch films.[21–27] To enhance this structure, sodium alginate is combined with another polymer, polyvinyl alcohol (PVA), which imparts a more plastic-like texture to the film.[24] In this work, we investigate the integration of additives to achieve a biofilm

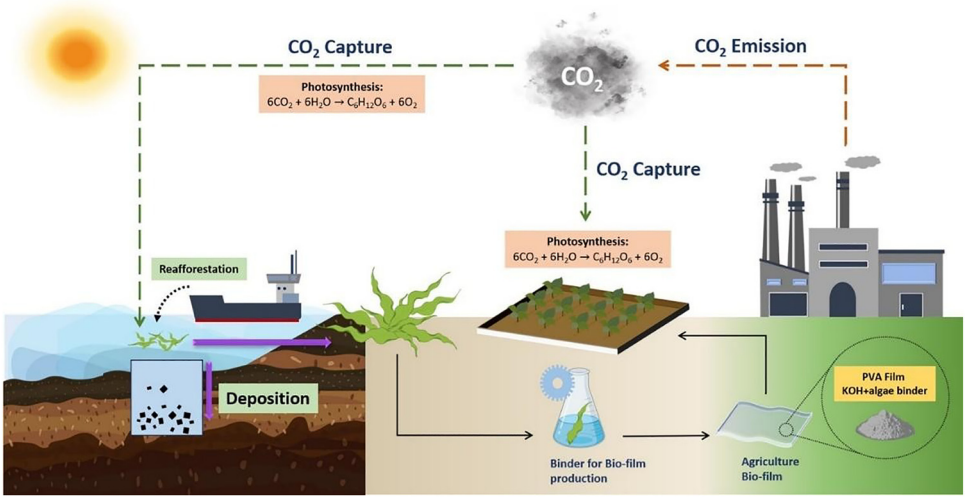

Fig. 1 Conceptual illustration of the circular pathway motivating this work: biomass-based CO_2 fixation and valorization into biodegradable agricultural films. CO_2 is captured *via* photosynthesis in marine algae (*Sargassum*) and terrestrial plants, converting CO_2 and H_2O into biomass. The resulting algae biomass is valorized as a sustainable precursor for biofilm production (sodium alginate binder), which is combined with recycled polyvinyl alcohol (PVA) to fabricate biodegradable agricultural films. This framework highlights the sustainability rationale of renewable feedstocks, reduced reliance on conventional plastics, and potential mitigation of plastic pollution in agricultural soils.

© 2026 The Author(s). Published by the Royal Society of Chemistry

Open Access Article. Published on 11 May 2026. Downloaded on 6/2/2026 12:52:24 PM. This article is licensed under a Creative Commons Attribution-NonCommercial 3.0 Unported Licence.

with specific functions and properties. The hydroxyl groups in PVA form hydrogen bonds with the carboxyl and hydroxyl groups in sodium alginate, resulting in a network that enhances the mechanical strength and flexibility of the film.[28,29] The combination of PVA and sodium alginate can form interpenetrating polymer networks (IPNs), where the two polymers interlace but are not covalently bonded. This structure can improve the film's properties, such as tensile strength, elasticity, and barrier properties.[30]

In this study, *Sargassum* biomass was valorized into sodium alginate (SA) and combined with recycled polyvinyl alcohol (PVA) to fabricate biodegradable mulch films containing glycerol (plasticizer) and zein (bioactive additive), followed by a beeswax surface coating to improve water resistance. Film performance was evaluated through thickness/appearance, water contact angle, tensile properties, UV-vis light shielding, structural/thermal characterization (FTIR, SEM, TGA/DTG), moisture interaction tests, outdoor biodegradation under natural rainfall and sunlight, and soil safety using OECD Guideline 207 with *Eisenia fetida*. The resulting films achieved a clear hydrophobicity improvement with beeswax coating (contact angle increasing from $\sim 74^\circ$ uncoated to $>100^\circ$ and up to $\sim 116^\circ$), tensile strength in the $\sim$8–13 MPa range depending on formulation and coating condition, strong UV blocking ($<1\%$ transmittance below 400 nm), complete outdoor degradation within $\sim$35 days for the double-side coated film, and 0% earthworm mortality, demonstrating a practical pathway to reduce reliance on conventional polyethylene mulch films.

Using *Sargassum* to achieve SDGs: this work aligns with SDG 12 (responsible production) and SDG 14 (marine resource management) by valorizing *Sargassum* into biodegradable agricultural materials.[39] It addresses challenges of marine waste management and soil degradation by converting brown algae, specifically *Sargassum*, into a biodegradable mulch film. By combining sodium alginate with recycled PVA, the study addresses the urgent need for alternatives to conventional plastic mulch films, which harm soil health and contribute to plastic pollution. The proposed biodegradable mulch film not only supports healthier soils through the gradual deposition of organic matter but also demonstrates a strong example of circular economy principles by transforming waste into value-added materials. The sustainability rationale and conceptual pathway from CO_2 fixation to biomass valorization and agricultural application are summarized in Fig. 1. Moreover, this sustainable solution contributes to climate action by reducing greenhouse gas emissions and enhancing long-term soil carbon storage.

Recycled polyvinyl alcohol (PVA) was selected as the blending polymer because its hydroxyl-rich backbone can form dense hydrogen-bonded networks with sodium alginate (SA), improving film-forming ability and flexibility while enabling upcycling of an industrial waste polymer stream. In contrast, replacing PVA with polylactic acid (PLA) would require fundamentally different processing (typically melt processing or organic-solvent casting), and PLA generally shows limited miscibility with alginate in the absence of compatibilizers, often leading to brittle structures or phase separation. Therefore, SA–PVA blending offers a water-processable route compatible with low-toxicity additives (glycerol, zein) and surface wax coating. The novelty of this work is the integrated pathway that combines *Sargassum*-derived SA with recycled PVA, zein antimicrobial functionality, and beeswax hydrophobic coating, followed by validation under outdoor exposure and standardized soil safety testing (OECD 207).

2. Experimental

2.1. Materials

Recycled PVA was received from Chung Cheng factory (Taiwan) as an industrial byproduct stream. Sodium alginate (SA) (Sigma-Aldrich; commercial grade; supplier did not report molecular weight), zein, potassium hydroxide, and ethanol were purchased from Sigma-Aldrich *via* UNI-ONWARD Corp. (Taipei, Taiwan). Glycerol (anhydrous) was purchased from J.T.Baker®. Beeswax and emulsifier were purchased from Shun Yi Chemical Co., Ltd (Taiwan). Deionized water was used throughout. The *Sargassum* referenced in this work corresponds to strandings from the great atlantic *Sargassum* belt (GASB) and motivates biomass valorization; in this study, commercial alginate was used to establish film performance, and future work will directly compare alginate extracted from *Sargassum* to commercial sources.

2.2. Preparation of films

Biodegradable mulch films were prepared in two stages: film formation and surface coating (Table 1).

Film formation: sodium alginate was dissolved in distilled water at 70 ± 5 °C for 40 min. In parallel, recycled solid PVA containing residual H_2SO_4 was dissolved in water at 90 ± 5 °C using a PVA-to-water ratio of 2 : 1. Once fully dissolved, the pH was adjusted to slightly basic conditions using aqueous KOH to improve polymer chain stability. The two polymer solutions were combined and magnetically stirred at 70 ± 5 °C until homogeneous. A sodium alginate-only control film (film C) was also prepared using the same procedure while omitting recycled PVA. This control isolates the effect of PVA blending on film performance. Film C provides a single-biopolymer

Table 1 Film formulations are summarized for clarity and replicability

Film	SA (g)	PVA (g)	Glycerol (wt% of polymer)	Zein (wt% of polymer)	Beeswax coating
A	5.0	2.5	7.5	5.0	Yes (top or both sides as specified)
B	5.0	2.5	7.5	0	Yes (top or both sides as specified)
C	5.0	0	7.5	5.0	Yes (top or both sides as specified)
D (PE)	—	—	—	—	Commercial black PE mulch film

Open Access Article. Published on 11 May 2026. Downloaded on 6/2/2026 12:52:24 PM. This article is licensed under a Creative Commons Attribution-NonCommercial 3.0 Unported Licence.

baseline but is more moisture-sensitive and less flexible than SA–PVA films, supporting the need for blending and surface coating. A 7.5 wt% plasticizer (glycerol) was added to enhance flexibility. Separately, 5 wt% zein was dissolved in 75% v/v ethanol at a 5% w/v concentration and incorporated into the polymer blend. The final mixture was poured into Petri dishes and dried in a vacuum oven at 45 ± 5 °C for 24 h, yielding water-sensitive hydrogel films.

Surface coating: once dried, films were cooled to room temperature and coated with a hydrophobic layer. To achieve a theoretical coating thickness of 25 μm, approximately 0.369 g of beeswax was applied per film (surface area: 154 cm^2; beeswax density: 0.96 g cm^{-3}). Beeswax was dissolved in 99.8% v/v ethanol at 70 ± 5 °C using a 1 : 25 beeswax-to-solvent weight ratio (9.225 g solvent), followed by 5 wt% emulsifier to ensure proper dispersion. The solution was evenly applied to the film surface and allowed to dry at room temperature, producing hydrophobic biodegradable mulch films entirely from non-toxic materials. Beeswax was selected because it is bio-based and solid at ambient conditions, enabling a stable hydrophobic barrier layer; in contrast, plant oils such as palm oil are typically liquid/semi-liquid and may migrate or wash off more readily without structural stabilization. Coating thickness was verified gravimetrically by measuring applied beeswax mass per unit area and converting to thickness using beeswax density, and cross-checked against the measured thickness increase after coating.

2.3. Physical properties

Thickness: film thickness was measured at multiple points using a digital caliper, and the average thickness was reported. Water contact angle measurements were performed using a Phoenix mini contact angle analyzer (Applied Micro Tech Inc.) at 20 ± 2 °C and 65 ± 10% RH. Five measurements per film were averaged. In general, water contact angles < 90° indicate a hydrophilic surface (better wetting), whereas angles > 90° indicate a hydrophobic surface (poorer wetting), with higher angles reflecting greater water repellency.

Mechanical properties: tensile strength and elongation at break were assessed using a Universal Testing Machine (Model M550-25AT). Specimens (40 × 20 mm^2) were tested in triplicate at a strain rate of 5 mm min^{-1} until fracture. Tensile strength (F) was calculated as:

$$F = \frac{f}{(w \times \mu)} \quad (1)$$

where F is the tensile strength (MPa), f is the force at break (N), w is the width of the sample (mm) and μ is the thickness of the sample (mm). The strain (%) was obtained by

$$\varepsilon = \frac{\delta}{L} \times 100\% \quad (2)$$

where, ε is the strain (%), δ is the length of stretch (mm), and L is the length of the sample (mm).

2.4. Structural and thermal characterization

The chemical structure, optical properties, surface morphology, and thermal stability of the films were comprehensively characterized. Chemical bonding was analyzed using FTIR spectroscopy (Tracer-100, ATR-GE mode, 1000–4000 cm^{-1}), while optical transmittance was measured with a UV-vis spectrophotometer (PerkinElmer Lambda 265, 200–800 nm), averaging five random measurements per sample. Surface and cross-sectional morphology were observed by SEM (JEOL JSM-IT800, 5 kV) on cryogenically fractured specimens coated with platinum (JEOL JEC-3000FC, 20 mV, 35 s). Thermal stability and decomposition behavior were evaluated by thermogravimetric analysis (TGA 550, TA Instruments) from 35 to 600 °C at a heating rate of 10 °C min^{-1} under a nitrogen flow of 20 mL min^{-1}.

2.5. Moisture sensitivity

Water absorption was evaluated under 30 ± 5% RH, 75 ± 5% RH, and ambient conditions (50 ± 30% RH). Films were pre-dried at 35 °C, weighed, exposed to humidity conditions, and reweighed after 1 and 2 weeks. Water absorption (%) was calculated as:

$$\text{Water absorption (\%)} = \left[\frac{(W_f - W_0)}{W_0}\right] \times 100\% \quad (3)$$

where W_f = final weight, W_0 = initial weight. Two-way ANOVA assessed the effect of film composition and humidity on water absorption.

Free water loss was measured on 2 × 2 cm^2 samples at 20 ± 5 °C, 45 ± 5 °C, and 60 ± 5 °C for over 48 h, recording weights at 2 h intervals for the first 6 h and then at 24 h and 48 h. Weight loss (%) was calculated as:

$$\text{Weight loss (\%)} = \left(\frac{W_0 - W_t}{W_0}\right) \times 100 \quad (4)$$

2.6. Biodegradation and soil toxicity

Outdoor biodegradation was performed by placing films on soil surfaces in rooftop plant beds at NTUST under natural sunlight, rainfall, and fluctuating temperatures (25 ± 10 °C). Soil toxicity was assessed using OECD Guideline 207 with *Eisenia fetida*, confirming that degradation products did not negatively impact soil health and supporting the films' role in sustainable agriculture. In this study, long-term outdoor durability was primarily governed by coating coverage (single- *vs.* double-sided), coating continuity/thickness and adhesion, moisture uptake from soil contact, tensile integrity under handling, and exposure to natural rainfall–sunlight and temperature fluctuations.

2.7. Statistical analysis

All experimental data were analyzed using Microsoft Excel 2016 and Origin 2024b. One-way and two-way ANOVA evaluated the effects of individual parameters and their interactions, with statistical significance defined at $p < 0.05$ (Fig. 2).

© 2026 The Author(s). Published by the Royal Society of Chemistry

Open Access Article. Published on 11 May 2026. Downloaded on 6/2/2026 12:52:24 PM.
This article is licensed under a Creative Commons Attribution-NonCommercial 3.0 Unported Licence.

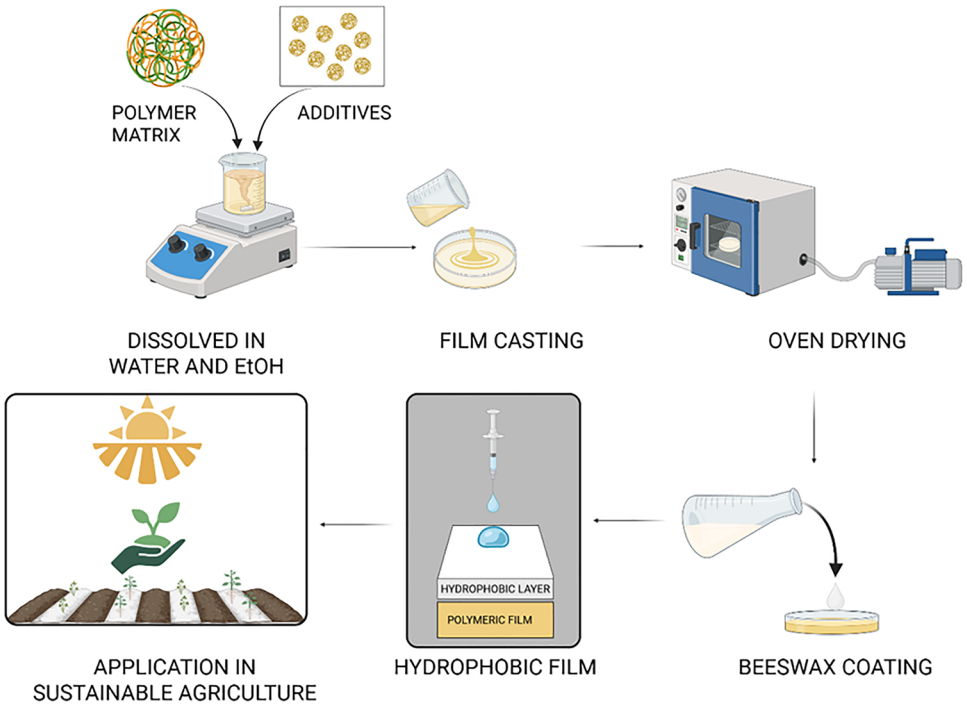

Fig. 2 Schematic diagram of the biodegradable film preparation and its application.

3. Results and discussion

The materials used in this study, SA and PVA, serve as the primary polymers, forming biodegradable films with enhanced mechanical properties. Glycerol was optimized as a plasticizer to improve flexibility, while zein was included as a functional bioactive additive; zein-based films/coatings have been reported to inhibit microbial growth, which is commonly attributed to protein-rich hydrophobic domains and interactions with microbial membranes. Beeswax coatings enhanced hydrophobicity and durability under outdoor agricultural conditions.[40,41] By optimizing polymer blends and additive concentrations, the films achieved improved mechanical strength, water resistance, UV protection, and controlled biodegradability, providing a sustainable alternative to conventional plastics.[42,43]

3.1. Film appearance, thickness, and hydrophobicity

Blending SA and PVA produced a light beige film, primarily due to SA, while dissolved PVA remained transparent.[42] The incorporation of zein shifted the colour toward cream, whereas zein-free mulch films retained higher transparency and greater homogeneity. SA-only films were uniform, while SA–PVA blends displayed vein-textured patterns caused by phase separation during drying.[43] These visual characteristics are not merely cosmetic; lighter-colored films can moderate soil heating and reduce UV transmission, while darker/opaque films absorb radiation and increase soil temperature.[44] Given the $<1\%$ UV transmittance we observed, combined with increased opacity after coating, the films are expected to provide effective weed suppression.

After applying the beeswax coating, the films developed a heterogeneous white crystalline surface, referred to as "wax blooms" (Fig. 3a), which increased opacity and introduced a discontinuous crystalline layer visible under SEM.[45,46] These dust-like particles, caused by the solidification of beeswax, could be brushed off partially, yet the films remained hydrophobic due to the beeswax layer beneath the surface. Research indicates that wax coatings such as beeswax increase opacity while altering mechanical resistance.[46] Thus, the coated films became opaque, reflecting the limited adhesion of beeswax to the polymer matrix.

Thickness measurements showed uncoated films averaged 0.25 ± 0.05 mm, while coated films measured 0.50 ± 0.05 mm. After brushing off the superficial wax bloom layer, the thickness decreased to $\sim$0.3 mm.[47,48] For comparison, Park, Friest, and Liu[47] reported thickness increases of 0.10–0.16 mm after beeswax coating, while conventional PE films typically measure $\sim$0.07 mm.[48]

Hydrophobicity increased significantly after coating. For uncoated films, the water contact angle was 73.6° (hydrophilic). With beeswax coating, the contact angle progressively increased from 99.20° (1 coat) to 116.54° (3 coats), as confirmed by one-way ANOVA (F (3,12) = 23.97, $p = 2.35 \times 10^{-5}$).[46] Fig. 3b illustrates this trend, while Fig. 3c and d show the contrast between uncoated (73.60°) and coated (116.17°) surfaces. Wax blooms locally reached $\sim$124.55°, though adherence was partial, resulting in some areas with lower values ($\sim 95° \pm 3°$). Since only the top side was coated, the backside of the biodegradable films exhibited lower hydrophobicity ($75° \pm 3°$; Fig. 3a), leaving them vulnerable to soil moisture.

In contrast, conventional PE films (film D) showed a uniform contact angle of $\sim$94° on both sides, lower than the front

Open Access Article. Published on 11 May 2026. Downloaded on 6/2/2026 12:52:24 PM.
This article is licensed under a Creative Commons Attribution-NonCommercial 3.0 Unported Licence.

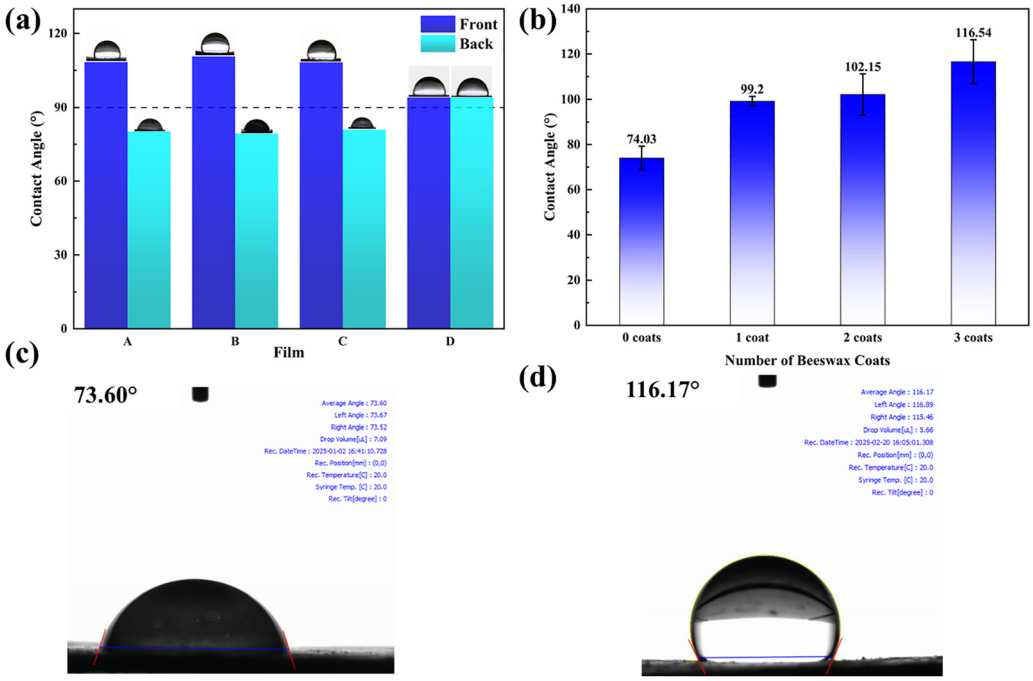

Fig. 3 (a) The contact angle for the different types of mulch films with the front side and backside. (b) Water contact angle measurements for biodegradable films with 0 to 3 layers of beeswax coating. Each bar shows the average value, and the error bars represent the standard deviation (n = 4). The contact angle of films before (c) being coated with beeswax at 73.60° and after (d) coating, hydrophobicity increases to 116.17°.

side of the coated biodegradable films but more evenly distributed. Thus, a biodegradable film coated with beeswax on both sides would last longer under outdoor exposure, balancing hydrophobicity and environmental degradability.

3.2. Mechanical properties (tensile strength, elongation at break)

Sodium alginate and PVA have many hydroxyl groups within their polymeric chains, allowing the formation of strong intermolecular hydrogen bonds.[49] Additionally, the carboxylic acid groups within sodium alginate contribute to its strong hydrophilic nature, facilitating hydrogen bonding with polar groups such as water and glycerol, thereby enhancing the film's mechanical properties.[50] Therefore, with the addition of glycerol as a plasticizer, variations in mechanical behavior were observed. Without plasticizer, both tensile strength and strain% were lowest in PVA-SA films (Fig. 4a), but increased progressively with higher glycerol concentrations. However, beyond 10% w/w glycerol, tensile strength decreased drastically, despite improved elongation. A similar trend was observed in films using only SA as the polymer (Fig. 4b), highlighting the polymers' sensitivity to hydrogen bonding. This suggests an optimal glycerol concentration is required to balance flexibility and strength. Increasing glycerol enhances flexibility through additional hydroxyl interactions, but may also increase water absorption and compromise mechanical integrity.[51]

After coating the films with beeswax, film thickness increased (see Section 3.1), affecting tensile strength calculations. Although the force (N) required to break the films increased, tensile strength (MPa) decreased because the load was distributed across the larger cross-sectional area. This effect arises from the doubling of film thickness, a phenomenon described as a 'size effect'.[52–54] Across our sets, uncoated films achieved ~13 MPa, whereas coated films dropped to ≥~8 MPa, representing a maximum reduction of ~38%. This decrease reflects thickness-driven effects rather than intrinsic polymer degradation.

In Fig. 4c, film A (PVA + SA) exhibited lower tensile strength than film C (SA only), consistent with Fig. 4a and b. This behavior is attributed to recycled PVA, which likely contains shorter polymer chains and weaker intermolecular bonding than sodium alginate. Film B, excluding zein, had the lowest tensile strength, indicating that zein not only functions as an antimicrobial additive but also contributes to mechanical reinforcement. Overall, coated films showed reduced tensile strength relative to uncoated counterparts, likely because beeswax interferes with stress transfer across the polymer matrix.

Film D (conventional PE) is much thinner yet mechanically superior due to the inherent chemical and physical properties of polyethylene. As reported by Ahmed *et al.*,[55] conventional plastics can persist in the environment for centuries, fragmenting into harmful microplastics.[56,57] As shown in Fig. 4d, film D demonstrated a strain of over 250%, approximately 40 times higher than biodegradable films A, B, and C, underscoring its persistence and durability.

3.3. Spectroscopic and optical properties (FTIR and UV analysis)

Fig. 5(a) shows the FTIR spectra of biodegradable films (film A, film B, and film C) compared with conventional polyethylene (film D). All three biodegradable films exhibited similar

© 2026 The Author(s). Published by the Royal Society of Chemistry

Open Access Article. Published on 11 May 2026. Downloaded on 6/2/2026 12:52:24 PM.
This article is licensed under a Creative Commons Attribution-NonCommercial 3.0 Unported Licence.

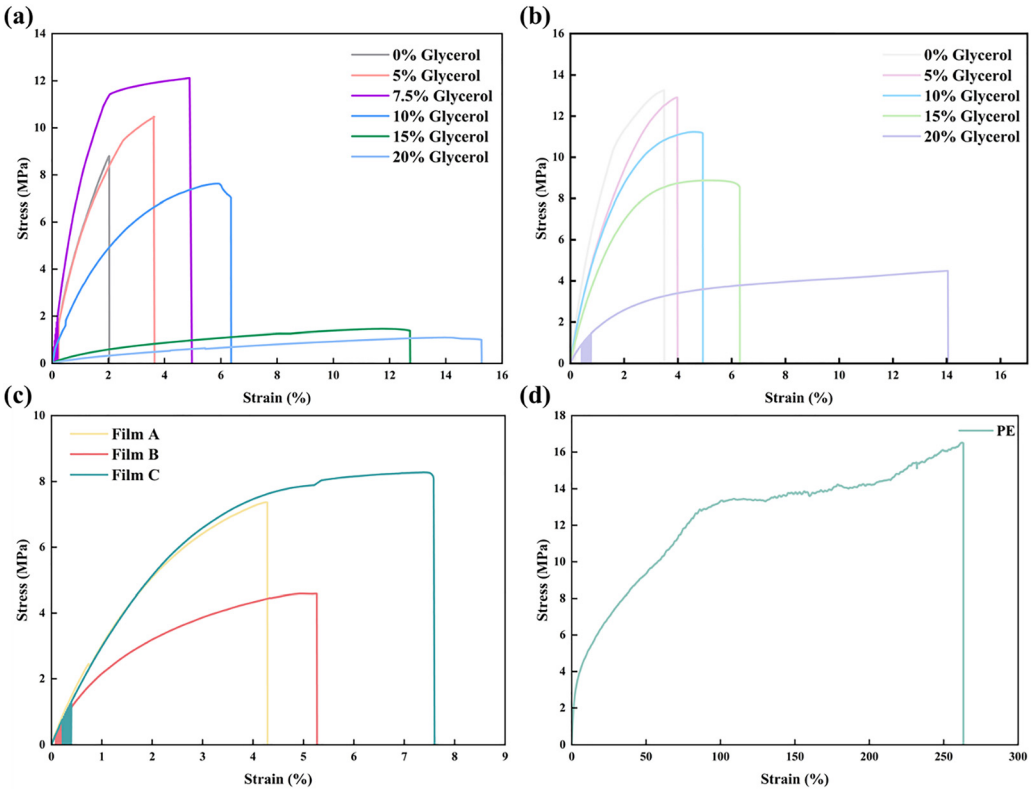

Fig. 4 Stress–strain of the polymer blend films made with PVA and SA films (a) and SA biopolymer alone (b), at varying glycerol concentrations to determine the optimum plasticizer content before hydrophobic coating. (c) Comparison of tensile properties of films A, B, and C. (d) Stress–strain curve of conventional PE film, exhibiting significantly higher strain at break compared to biodegradable films.

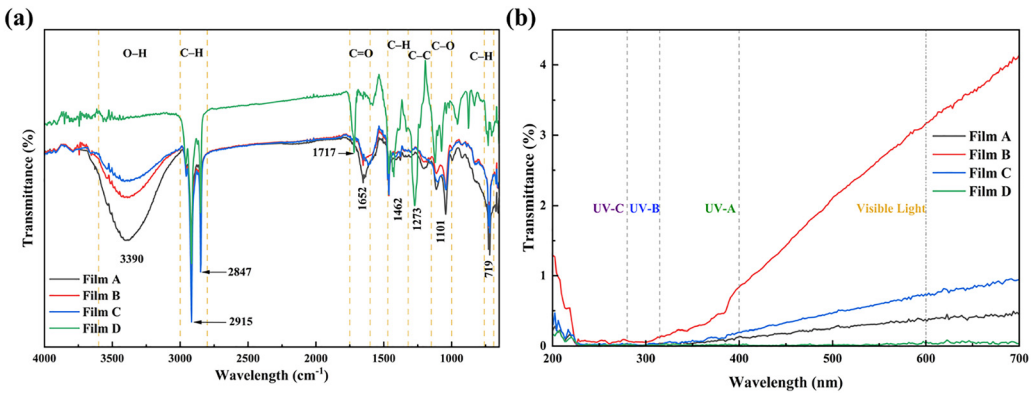

Fig. 5 (a) FTIR spectra of biodegradable polymer films (film A, film B, film C) compared with conventional polyethylene (PE) film (film D). Characteristic absorption bands include O–H stretching (~3390 cm^{-1}), C–H stretching (~2915 and 2847 cm^{-1}), and C=O stretching (~1652 cm^{-1} for biodegradable films, ~1717 cm^{-1} for PE film). Peaks at ~1462 cm^{-1}, ~1101 cm^{-1}, and ~719 cm^{-1} correspond to C–H bending, C–O–C stretching, and C–H rocking vibrations, respectively. Dashed vertical lines and arrows highlight the principal functional groups and their associated vibrations. (b) The transmittance of films A–B under the 200–700 nm range.

absorption profiles due to shared components such as sodium alginate, PVA, glycerol, and zein. A broad band between 3200–3550 cm^{-1} (centered ~3390 cm^{-1}) corresponds to O–H stretching from hydrogen bonding between hydroxyl groups in PVA, alginate, and glycerol. The presence of multiple hydroxyl groups in PVA and glycerol confirms their roles in plasticization and polymer chain bridging, improving mechanical strength.[51,58,59] Conversely, polyethylene, lacking hydroxyl groups, showed no absorption in this region, consistent with its purely covalent, hydrophobic nature.[60,61]

Characteristic C–H stretching vibrations appeared at 2915 and 2847 cm^{-1} for all films, while C=O stretching occurred at ~1652 cm^{-1} for films A–B and shifted to 1617 cm^{-1} in film C, indicating interactions between alginate carbonyls and zein

Open Access Article. Published on 11 May 2026. Downloaded on 6/2/2026 12:52:24 PM. This article is licensed under a Creative Commons Attribution-NonCommercial 3.0 Unported Licence.

residues. In contrast, film D exhibited a distinct peak at 1717 cm^{-1}, attributable to oxidative degradation products in polyethylene.[62–64] Additional bands were observed in the fingerprint region: 1462 cm^{-1} (C–H bending), 1101–1042 cm^{-1} (C–O–C and C–O stretching), and 719 cm^{-1} (C–H rocking). A unique 1274 cm^{-1} absorption in film D suggests ester/alcohol additives in PE films.[65] Overall, the FTIR spectra confirm that glycerol, zein, and beeswax only induce physical blending and hydrogen bonding rather than covalent bond formation.

Fig. 5(b) illustrates UV-visible transmittance. All biodegradable films demonstrated excellent UV-blocking (<1% transmittance between 200–400 nm), comparable to polyethylene. Above 350 nm, film C showed a slight transmittance increase (~4%) due to zein incorporation. The strong UV-attenuation effect is attributed to aromatic amino acids (tyrosine, phenylalanine) in zein, along with the intrinsic UV-protective roles of alginate and PVA.[24,66,67] Notably, film D (black PE mulch film) showed 0% transmittance throughout, while films A and C closely resembled its behavior in the visible region (<4%). These findings highlight the UV-protective function of biodegradable films, making them suitable for agricultural mulch applications where light regulation suppresses weed germination and controls soil temperature.[24,68–72] We additionally note that weed suppression depends on reducing visible/PAR transmission (400–700 nm) and overall opacity; therefore, UV blocking alone is not sufficient, and the visible-range transmittance/opacity should be considered when interpreting weed-control potential.

3.4. Film morphology and thermal stability

The structural and thermal properties of the biodegradable films were evaluated to understand their performance for agricultural mulch applications. SEM analysis revealed surface and cross-sectional morphologies (Fig. S2). The surface of beeswax-coated films (Fig. S2a) displayed mostly uniform regions with rough patches corresponding to residual wax blooms, while smoother areas indicated where wax had been removed. Small pores were observed, facilitating air transport essential for soil aeration and photosynthesis. Cross-sectional images (Fig. S2b) distinguished the top beeswax layer from the polymeric matrix blend, which appeared homogenized, indicating effective bonding between polymer chains. In contrast, conventional PE film (Fig. S2c) exhibited a less uniform morphology due to the absence of coating. Increasing glycerol content enhanced homogenization (Fig. S2d–f), with films containing 20% w/w glycerol showing smoother surfaces than those without, consistent with glycerol's plasticizing effect *via* hydrogen bonding.[51,73,74] However, excessive glycerol increases hydroxyl content and water sensitivity, requiring careful optimization.[75,76]

Thermal behavior, assessed by TGA and DTG (Fig. S3), showed multi-step degradation for biodegradable films (films A–C) and a simpler, delayed profile for PE film (film D).[56] Initial weight loss below 100 °C was attributed to moisture evaporation and low-molecular-weight volatiles, mainly glycerol.[51,67] Film A (PVA + SA + zein + beeswax) exhibited three degradation stages: an initial loss of 15.08% at ~184 °C due to moisture, a major loss of 39.39% at 217.74 °C from degradation of organic components (sodium alginate, low-molecular-weight PVA, glycerol, zein, beeswax), and a final 14.99% loss near 600 °C corresponding to carbonization of stable polymer fragments. The residue at 600 °C (30.88%) likely resulted from crosslinked zein-polysaccharide networks, indicating moderate thermal stability suitable for mulch films. Zein enhanced structural rigidity *via* protein-network crosslinking.[77,78] Film B, without zein, degraded at a slightly lower onset temperature with reduced residue (23.09%), reflecting diminished thermal integrity. Film C, composed solely of sodium alginate, degraded rapidly between 181–262 °C, with a DTG peak at 219.82 °C; although char residue was high (30.61%), absence of PVA limited overall matrix stability.[79–81] PE film degraded over a narrower temperature range with minimal early-stage residue, demonstrating its non-biodegradable nature.

Overall, SEM and TGA analyses indicate that polymer composition and additive incorporation critically influence microstructure and thermal properties. Homogenized matrices with proper additives improve both structural and thermal stability, while beeswax and glycerol further modulate surface features and thermal behavior, enabling tunable properties for environmental and agricultural applications.

3.5. Moisture absorption and retention behavior

The interaction of biodegradable films with water was evaluated under varying humidity and temperature conditions to mimic real-world applications. Both film A (PVA + SA) and film C (SA only) contain hydrophilic polymers with hydroxyl groups, making them sensitive to environmental moisture.[28,66,82–85] The water absorption percentages under different relative humidity (RH) after one and two weeks are summarized in Table S1 and illustrated in Fig. 6a. Films exposed to 30% RH ±5% RH showed the highest weight loss, particularly film A1 (−19.0%), whereas films at 75% RH ±5% RH, notably film C3, exhibited slight weight gain (1.5%). This highlights that both humidity and polymer composition influence moisture uptake or loss, with most changes occurring during the first week. Film A lost more weight than film C across all conditions, likely due to PVA's higher hydrophilicity.[84–87] Film C's better stability is attributed to its more cross-linked alginate structure with ionic bonds.[88,89]

Fig. 6b shows the weight variation of the films over time during RH exposure. Films under 30% RH ±5% RH had the highest water loss, with film A losing more than film C, while at 50% ±30% RH, differences were smaller. Under 75% RH ±5% RH, film A still lost weight, but film C absorbed moisture, demonstrating better retention. Most water absorption/desorption occurred in the first week, after which the films reached equilibrium.

The temperature-dependent free water loss was also measured at 20 °C ± 5 °C, 45 °C ± 5 °C, and 60 °C ± 5 °C (Fig. 6c and d). Rapid weight reduction occurred at 45 °C and more drastically at 60 °C, mostly within the first 2 hours. At room temperature, weight remained nearly constant, with minor fluctuations likely due to humidity.[90] Film A consistently retained more water

© 2026 The Author(s). Published by the Royal Society of Chemistry

Open Access Article. Published on 11 May 2026. Downloaded on 6/2/2026 12:52:24 PM. This article is licensed under a Creative Commons Attribution-NonCommercial 3.0 Unported Licence.

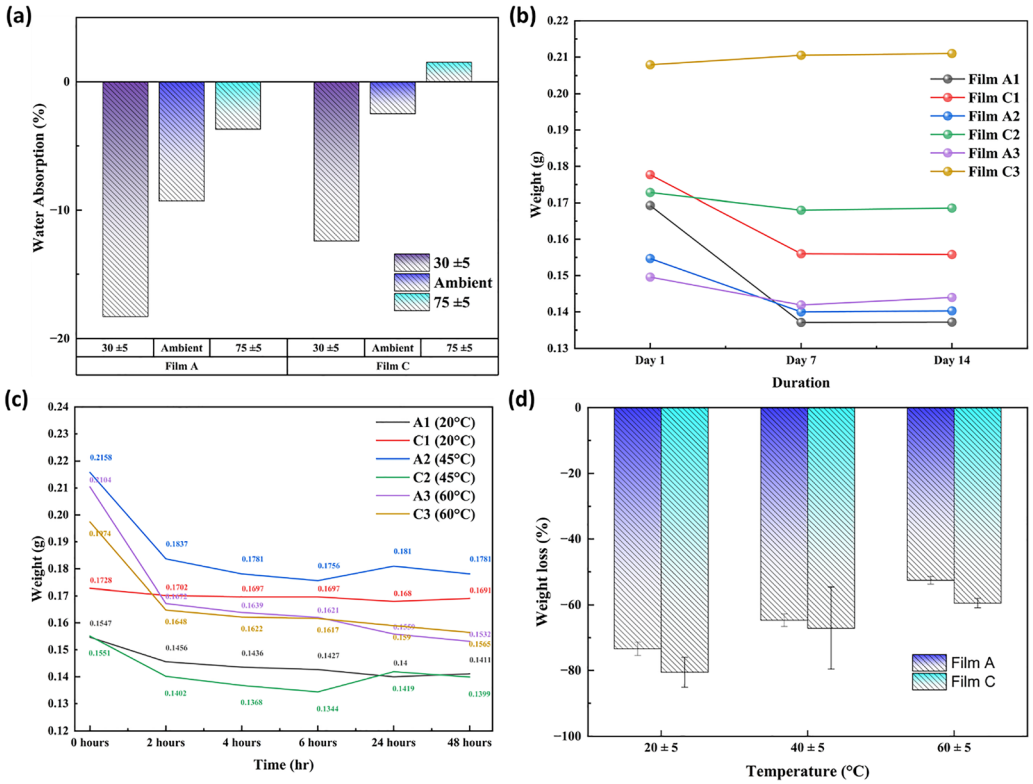

Fig. 6 Moisture absorption and retention behavior of biodegradable films. (a) Water absorption (%) of film A (PVA + SA) and film C (SA only) after two weeks under different relative humidity (RH) conditions. (b) Weight (g) variation of the films over time during RH exposure (day 1, week 1, week 2). (c) Weight (g) of films measured over time under three temperature conditions (20 °C, 45 °C, 60 °C). (d) Free water loss (%) of film A and film C after 48 hours under the three temperature conditions.

than film C across all temperatures, especially at 20 °C and 60 °C, indicating PVA improves water retention and stability.[82,83,91]

A two-way ANOVA showed a significant difference (p = 0.007) between film A and film C, confirming that polymer composition affects water retention more than temperature (p = 0.644) or their interaction (p = 0.462). Film A's polymeric blend is therefore more suitable for outdoor use.

3.6. Biodegradation and soil toxicity

The biodegradation performance of the films was evaluated under real outdoor conditions to simulate their practical application as mulch films. The films were placed on the rooftop of NTUST (Fig. 7a), an open area exposed to direct sunlight, wind, and rainfall. Initially, the films were coated with beeswax only on the top surface, leaving a hydrophilic underside in contact with soil. It was hypothesized that this hydrophilic surface could retain moisture beneficial for plants. However, exposure to rainfall resulted in rapid water penetration into the film matrix, compromising mechanical integrity and causing significant biodegradation within 2 weeks (Fig. 7b1–b3). The configuration used here is surface exposure on soil; half-buried/buried configurations will be included in future work to better simulate agricultural coverage conditions.

To improve film longevity, both sides were subsequently coated with beeswax, increasing water resistance and slowing biodegradation. These double-sided films remained largely intact after 2 weeks of exposure (Fig. 7c2). Despite intermittent rainfall, water slowly penetrated the films, initiating gradual degradation. By 5 weeks, the films had showed near-complete breakdown by the final time point, leaving only small residual white beeswax fragments on the soil surface (Fig. 7c4). These observations demonstrate that hydrophobic surface modification can enhance film durability while maintaining complete biodegradability under natural environmental conditions. The observed sequence is consistent with water ingress weakening the hydrophilic matrix, followed by microbial assimilation of polysaccharide/protein components once coating continuity is disrupted.

Following biodegradation, soil toxicity was assessed to ensure environmental safety. Acute toxicity tests were performed according to OECD Guideline 207 using the earthworm *Eisenia fetida*. This work evaluates outdoor surface exposure and short-term ecotoxicity and does not constitute certification testing to compostability/biodegradation standards (*e.g.*, EN 13432, ASTM D6400, ISO 17088), which will require controlled-condition biodegradation, disintegration, and ecotoxicity endpoints in future studies.

Priority research directions: future work should focus on (i) scale-up of film casting and beeswax coating to ensure thickness uniformity and reproducibility, (ii) improving wax–substrate adhesion and minimizing surface bloom/whitening to maintain durable hydrophobicity, (iii) validating performance under broader field conditions (different soils, climates, and

Open Access Article. Published on 11 May 2026. Downloaded on 6/2/2026 12:52:24 PM.
This article is licensed under a Creative Commons Attribution-NonCommercial 3.0 Unported Licence.

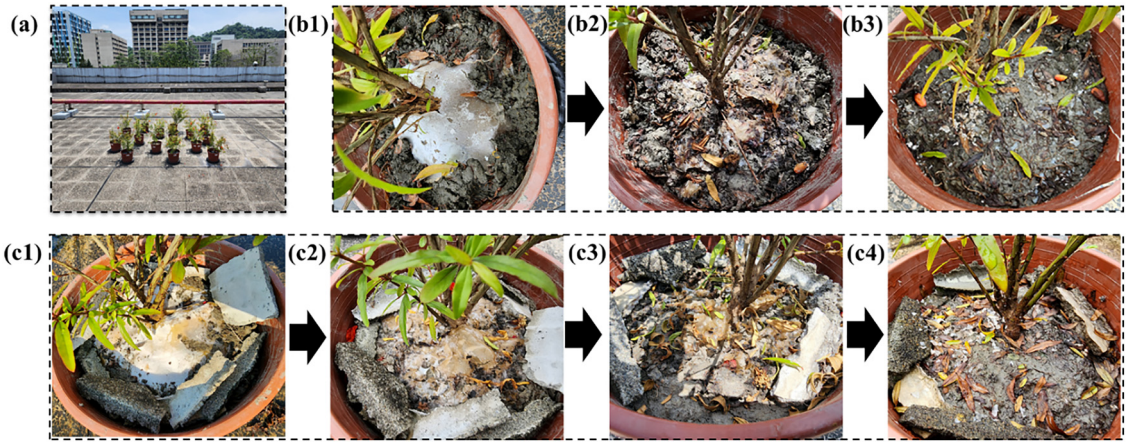

Fig. 7 Outdoor biodegradation of biodegradable films exposed to natural rainfall and sunlight. (a) The rooftop of a building at NTUST used for the outdoor biodegradation experiment. (b1) Biodegradable films coated only on the top side at the initial stage, (b2) after 1 week, and (b3) after 2 weeks of exposure. (c1) Biodegradable films coated on both sides at the initial stage, (c2) after 2 weeks, (c3) after 4 weeks, and (c4) after 5 weeks of exposure.

cropping practices), (iv) extending environmental safety testing beyond acute endpoints through longer-term ecotoxicity (*e.g.*, chronic earthworm exposure) and plant response assays, and (v) integrating life cycle assessment and techno-economic analysis to quantify environmental and economic trade-offs and guide deployment decisions.

4. Conclusions

This study demonstrates a sustainable pathway for transforming invasive *Sargassum* biomass into biodegradable mulch films by combining sodium alginate (SA) with recycled polyvinyl alcohol (PVA), glycerol, zein, and a beeswax surface coating. The resulting films exhibited mechanical robustness (8–13 MPa tensile strength), tunable hydrophobicity (water contact angle up to 116.5°), and strong UV-blocking capacity (<1% transmittance below 400 nm). Structural and thermal analyses supported formation of hydrogen-bonded polymer networks with enhanced thermal stability. Moisture interaction tests further indicated improved moisture retention of SA–PVA blends relative to SA-only films. Outdoor exposure trials verified complete biodegradation within 35 days, and OECD Guideline 207 soil toxicity assays showed 0% earthworm mortality, supporting soil compatibility.

By eliminating glutaraldehyde, valorizing marine biomass, and incorporating recycled PVA, these films demonstrate a circular-material pathway and provide a viable alternative to conventional petroleum-based mulch films for applications where controlled durability followed by environmental breakdown is required. Overall, this work demonstrates a practical pathway to valorize invasive *Sargassum* into biodegradable agricultural films and reduce reliance on conventional petroleum-based mulch plastics.

Conflicts of interest

The authors declare that they have no known competing financial interests or personal relationships that could have appeared to influence the work reported in this paper.

Data availability

The data supporting the findings of this study are available within the article and its supplementary information (SI). Supplementary information is available. See DOI: https://doi.org/10.1039/d5ma01298h.

Additional raw data generated and analyzed during the current study are available from the corresponding author upon reasonable request.

Acknowledgements

This study was supported by the Ministry of Education under the "University Social Responsibility Project LET'S Go!."

References

1 G. Chataut, B. Bhatta, D. Joshi, K. Subedi and K. Kafle, Greenhouse gases emission from agricultural soil: A review, *J. Agric. Food Res.*, 2023, **11**, 100533.
2 N. M. Modak, D. K. Ghosh, S. Panda and S. S. Sana, Managing green house gas emission cost and pricing policies in a two-echelon supply chain, *CIRP J. Manuf. Sci. Technol.*, 2018, **20**, 1–11.
3 Statista, Global CO_2 Emissions from Fossil Fuels and Industry (2002–2050), Ian Tiseo, 2024.
4 Statista, Annual carbon dioxide (CO_2) emissions worldwide from 1940 to 2024, 2024.
5 E. National Academies of Sciences, and Medicine, Getting to Net-Zero Emissions by 2050, 2021. https://nap.nationalacademies.org/resource/other/dels/net-zero-emissions-by-2050/. (Accessed 2024).
6 U.S.E.P. Agency, Great Atlantic *Sargassum* Belt (GASB), 2024. https://www.epa.gov/habs/great-atlantic-sargassum-belt-gasb. (Accessed 2024).
7 H. A. Oxenford, S.-A. Cox, B. I. van Tussenbroek and A. Desrochers, Challenges of Turning the *Sargassum* Crisis

© 2026 The Author(s). Published by the Royal Society of Chemistry

Open Access Article. Published on 11 May 2026. Downloaded on 6/2/2026 12:52:24 PM. This article is licensed under a Creative Commons Attribution-NonCommercial 3.0 Unported Licence.

into Gold: Current Constraints and Implications for the Caribbean, *Phycology*, 2021, 27–48.
8 M. Starling, Caribbean startups are turning excess seaweed into an agroecology solution, 2024. https://news.mongabay.com/2024/04/caribbean-startups-are-turning-excess-seaweed-into-an-agroecology-solution/. (Accessed 2024).
9 C. G. Lopresto, R. Paletta, P. Filippelli, L. Galluccio, C. de la Rosa, E. Amaro, U. Jáuregui-Haza and J. A. de Frias, *Sargassum* Invasion in the Caribbean: An Opportunity for Coastal Communities to Produce Bioenergy Based on Biorefinery—An Overview, *Waste Biomass Valorization*, 2022, **13**(6), 2769–2793.
10 N. Ramli, M. Norkhairunnisa, Y. Ando, K. Abdan and Z. Leman, Advanced Polymer Composite for Aerospace Engineering Applications, in *Advanced Composites in Aerospace Engineering Applications*, ed. N. Mazlan, S. M. Sapuan and R. A. Ilyas, Springer International Publishing, Cham, 2022, pp. 1–21.
11 Z. Wu, J. He, H. Yang and S. Yang, Progress in Aromatic Polyimide Films for Electronic Applications: Preparation, Structure and Properties, *Polymers*, 2022, **14**(6), 1269.
12 J. G. Drobny, 1 – Introduction, in *Applications of Fluoropolymer Films*, ed. J. G. Drobny, William Andrew Publishing, 2020, pp. 3–38.
13 P. Balakrishnan, M. S. Thomas, L. A. Pothen, S. Thomas and M. S. Sreekala, Polymer Films for Packaging, in *Encyclopedia of Polymeric Nanomaterials*, ed. S. Kobayashi and K. Müllen, Springer Berlin Heidelberg, Berlin, Heidelberg, 2014, pp. 1–8.
14 I. Wojnowska-Baryła, K. Bernat and M. Zaborowska, Plastic Waste Degradation in Landfill Conditions: The Problem with Microplastics, and Their Direct and Indirect Environmental Effects, *Int. J. Environ. Res. Public Health*, 2022, **19**(20), 13223.
15 H. Doh, K. D. Dunno and W. S. Whiteside, Preparation of novel seaweed nanocomposite film from brown seaweeds Laminaria japonica and *Sargassum* natans, *Food Hydrocolloids*, 2020, **105**, 105744.
16 S. Kasirajan and M. Ngouajio, Polyethylene and biodegradable mulches for agricultural applications: a review, *Agron. Sustainable Dev.*, 2012, **32**(2), 501–529.
17 M. Abe, K. Kobayashi, N. Honma and K. Nakasaki, Microbial degradation of poly(butylene succinate) by Fusarium solani in soil environments, *Polym. Degrad. Stab.*, 2010, **95**(2), 138–143.
18 G. Amare and B. Desta, Coloured plastic mulches: impact on soil properties and crop productivity, *Chem. Biol. Technol. Agric.*, 2021, **8**(1), 4.
19 H. S. El-Beltagi, A. Basit, H. I. Mohamed, I. Ali, S. Ullah, E. A. R. Kamel, T. A. Shalaby, K. M. A. Ramadan, A. A. Alkhateeb and H. S. Ghazzawy, Mulching as a Sustainable Water and Soil Saving Practice in Agriculture: A Review, *Agronomy*, 2022, **12**(8), 1881.
20 T. M. Thompson, B. R. Young and S. Baroutian, Pelagic *Sargassum* for energy and fertiliser production in the Caribbean: A case study on Barbados, *Renewable Sustainable Energy Rev.*, 2020, **118**, 109564.
21 G. D. T. M. Jayasinghe, B. K. K. K. Jinadasa and N. A. G. Sadaruwan, Pathway of sodium alginate synthesis from marine brown algae, Sargassum wightii from Sri Lanka, *Discover Food*, 2022, **2**(1), 2.
22 S. Saji, A. Hebden, P. Goswami and C. Du, A Brief Review on the Development of Alginate Extraction Process and Its Sustainability, *Sustainability*, 2022, **14**(9), 5181.
23 S. H. Rashedy, M. S. M. Abd El Hafez, M. A. Dar, J. Cotas and L. Pereira, Evaluation and Characterization of Alginate Extracted from Brown Seaweed Collected in the Red Sea, *Appl. Sci.*, 2021, **11**(14), 6290.
24 W. Su, Z. Yang, H. Wang, J. Fang, C. Li, G. Lyu and H. Li, Synergistic Effect of Sodium Alginate and Lignin on the Properties of Biodegradable Poly(vinyl alcohol) Mulch Films, *ACS Sustainable Chem. Eng.*, 2022, **10**(36), 11800–11814.
25 A. Mohammed, A. Gaduan, P. Chaitram, A. Pooran, K.-Y. Lee and K. Ward, Sargassum inspired, optimized calcium alginate bioplastic composites for food packaging, *Food Hydrocolloids*, 2023, **135**, 108192.
26 X. Zhang, D. Gao, W. Luo, N. Xiao, G. Xiao, Z. Li and C. Liu, Hemicelluloses-based sprayable and biodegradable pesticide mulch films for Chinese cabbage growth, *Int. J. Biol. Macromol.*, 2023, **225**, 1350–1360.
27 D. Wang, Z. Song, X. Kong, J. Wu, J. Xu, J. Ye, Y. Zhu, R. Zhang, X. Ma, G. Li, S. Xu and D. Cai, Fabrication of biodegradable mulch film based on polylactic acid waste liquid, *Chem. Eng. J.*, 2025, **513**, 163113.
28 Y. Xie, Y. Pan and P. Cai, Hydroxyl crosslinking reinforced bagasse cellulose/polyvinyl alcohol composite films as biodegradable packaging, *Ind. Crops Prod.*, 2022, **176**, 114381.
29 Z. Huang, Y. Zhang, C. Zhang, F. Yuan, H. Gao and Q. Li, Lignin-Based Composite Film and Its Application for Agricultural Mulching, *Polymers*, 2024, **16**(17), 2488.
30 S. Bongiovanni Abel, C. A. Busatto, F. Karp, D. Estenoz and M. Calderón, Weaving the next generation of (bio)materials: Semi-interpenetrated and interpenetrated polymeric networks for biomedical applications, *Adv. Colloid Interface Sci.*, 2023, **321**, 103026.
31 S. Bandopadhyay, L. Martin-Closas, A. M. Pelacho and J. M. DeBruyn, Biodegradable Plastic Mulch Films: Impacts on Soil Microbial Communities and Ecosystem Functions, *Front. Microbiol.*, 2018, **9**, 819.
32 R. Saberi Riseh, Advancing agriculture through bioresource technology: The role of cellulose-based biodegradable mulches, *Int. J. Biol. Macromol.*, 2024, **255**, 128006.
33 Y. Yang, P. Li, J. Jiao, Z. Yang, M. Lv, Y. Li, C. Zhou, C. Wang, Z. He, Y. Liu and S. Song, Renewable sourced biodegradable mulches and their environment impact, *Sci. Hortic.*, 2020, **268**, 109375.
34 M. Stevenson, J. Long, A. Seyfoddin, P. Guerrero, K. D. L. Caba and A. Etxabide, Characterization of ribose-induced crosslinking extension in gelatin films, *Food Hydrocolloids*, 2020, **99**, 105324.
35 F. Huang, Q. Zhang, L. Wang, C. Zhang and Y. Zhang, Are biodegradable mulch films a sustainable solution to

Open Access Article. Published on 11 May 2026. Downloaded on 6/2/2026 12:52:24 PM. This article is licensed under a Creative Commons Attribution-NonCommercial 3.0 Unported Licence.

microplastic mulch film pollution? A biogeochemical perspective, *J. Hazard. Mater.*, 2023, **459**, 132024.
36 E. Liu, L. Zhang, W. Dong and C. Yan, Biodegradable plastic mulch films in agriculture: feasibility and challenges, *Environ. Res. Lett.*, 2021, **16**(1), 011004.
37 Z. Song, L. Zhao, J. Bi, Q. Tang, G. Wang and Y. Li, Classification of Degradable Mulch Films and Their Promotional Effects and Limitations on Agricultural Production, *Agriculture*, 2024, **14**(8), 1235.
38 Z. Liu, C. Zhao, N. Zhang, J. Wang, Z. Li, Y. Uwiragiye, N. Fallah, T. W. Crowther, Y. Huang, Y. Huang, Y. Xu, S. Zhang, Y. Kuzyakov, K. H. M. Siddique, Z. Jia, Z. Cai, S. X. Chang, M. Xu, C. Müller and Y. Cheng, Degradable film mulching increases soil carbon sequestration in major Chinese dryland agroecosystems, *Nat. Commun.*, 2025, **16**(1), 5029.
39 n.d, The 17 goals. https://sdgs.un.org/goals.
40 J. E. Gough, C. A. Scotchford and S. Downes, Cytotoxicity of glutaraldehyde crosslinked collagen/poly(vinyl alcohol) films is by the mechanism of apoptosis, *J. Biomed. Mater. Res.*, 2002, **61**(1), 121–130.
41 H.-W. Leung, Ecotoxicology of Glutaraldehyde: Review of Environmental Fate and Effects Studies, *Ecotoxicol. Environ. Saf.*, 2001, **49**(1), 26–39.
42 Y. L. Han, Q. Xu, Z. Q. Lu and J. Y. Wang, Preparation of transparent zein films for cell culture applications, *Colloids Surf., B*, 2014, **120**, 55–62.
43 C. M. Chaléat, P. J. Halley and R. W. Truss, Study on the phase separation of plasticised starch/poly(vinyl alcohol) blends, *Polym. Degrad. Stab.*, 2012, **97**(10), 1930–1939.
44 M. Ambrosi, M. Raudino, G. Pieraccini, C. Corti, A. Tenorio-Alfonso and I. Martínez, Understanding the formation of efflorescence on beeswax models housed at the Natural History Museum of Florence, *J. Cult. Herit.*, 2023, **62**, 143–150.
45 S. Shi, X. Xu, Y. Ren, H. Zhang, X. Du, H. Li and X. Xia, Beeswax coating improves the hydrophobicity of sodium alginate/anthocyanin/cellulose nanocrystal indicator film, *Food Hydrocolloids*, 2023, **144**, 108930.
46 S. Galus, M. Gaouditz, H. Kowalska and F. Debeaufort, Effects of Candelilla and Carnauba Wax Incorporation on the Functional Properties of Edible Sodium Caseinate Films, *Int. J. Mol. Sci.*, 2020, **21**(24), 9349.
47 N. Park, M. A. Friest and L. Liu, Enhancing the properties of polyvinyl alcohol films by blending with corn stover-derived cellulose nanocrystals and beeswax, *Polymers*, 2023, **15**(21), 4321.
48 G. M. Glenn, W. Orts, S. Imam, B.-S. Chiou and D. F. Wood, Starch Plastic Packaging and Agriculture Applications, in *Starch Polymers*, ed. P. J. Halley and L. Avérous, Elsevier, Amsterdam, 2014, ch. 15, pp. 421–452.
49 Z. Ma, Y. Ma, L. Qin, J. Liu and H. Su, Preparation and characteristics of biodegradable mulch films based on fermentation industry wastes, *Int. Biodeterior. Biodegrad.*, 2016, **111**, 54–61.
50 L. Hou and P. Wu, Exploring the hydrogen-bond structures in sodium alginate through two-dimensional correlation infrared spectroscopy, *Carbohydr. Polym.*, 2019, **205**, 420–426.
51 J. Tarique, S. M. Sapuan and A. Khalina, Effect of glycerol plasticizer loading on the physical, mechanical, thermal, and barrier properties of arrowroot (Maranta arundinacea) starch biopolymers, *Sci. Rep.*, 2021, **11**(1), 13900.
52 M. Soazo, A. C. Rubiolo and R. A. Verdini, Effect of drying temperature and beeswax content on physical properties of whey protein emulsion films, *Food Hydrocolloids*, 2011, **25**(5), 1251–1255.
53 L. Yang and L. Lu, The influence of sample thickness on the tensile properties of pure Cu with different grain sizes, *Scr. Mater.*, 2013, **69**(3), 242–245.
54 I. U. Fitriana, E. Rochima, I. Rostini and R. I. Pratama, Effect of Beeswax Addition in the Mechanical and Antimicrobial Properties of Edible Film Based on Fish Gelatin and Nanochitosan: A Review, *J. Mater. Sci. Res. Rev.*, 2023, **6**(2), 126–140.
55 R. Ahmed, A. K. Hamid, S. A. Krebsbach, J. He and D. Wang, Critical review of microplastics removal from the environment, *Chemosphere*, 2022, **293**, 133557.
56 Q. Tan, L. Yang, F. Wei, Y. Chen and J. Li, Comparative life cycle assessment of polyethylene agricultural mulch film and alternative options including different end-of-life routes, *Renewable Sustainable Energy Rev.*, 2023, **178**, 113239.
57 R. Bai, Z. Li, Q. Liu, Q. Liu, J. Cui and W. He, The reciprocity principle in mulch film deterioration and microplastic generation, *Environ. Sci.: Processes Impacts*, 2024, **26**(1), 8–15.
58 L. D. Mathews, J. C. Capricho, N. Salim, J. Parameswaranpillai, K. Moinuddin and N. Hameed, Intrinsically modified self-extinguishing fire-retardant epoxy resin using boron-polyol complex, *J. Polym. Res.*, 2023, **30**(7), 271.
59 N. Nordin, S. H. Othman, S. A. Rashid and R. K. Basha, Effects of glycerol and thymol on physical, mechanical, and thermal properties of corn starch films, *Food Hydrocolloids*, 2020, **106**, 105884.
60 X. Dong, D. Hu, H. Wang, Y. Huang, S. Long, G. Zhang and X. Li, Mechanical characterizations, recyclability of thermoplastics through melt grafting a dynamic covalent network onto polyethylene, *Polym. Test.*, 2023, **122**, 108005.
61 S.-J. Park and M.-K. Seo, Element and Processing, in *Interface Science and Technology*, ed. S.-J. Park and M.-K. Seo, Elsevier, 2011, ch. 6, pp. 431–499.
62 T. Shahsavari-Badvestani, R. Jahanmardi, M.-I. Tayouri and M. Fathi, Acceleration of thermo-oxidative degradation of high-density polyethylene using oxidized polyethylene, *Polym. Degrad. Stab.*, 2023, **203**, 110108.
63 Y. Yamamoto, H. Hoshina and H. Sato, Differences in Intermolecular Interactions and Flexibility between Poly(ethylene terephthalate) and Poly(butylene terephthalate) Studied by Far-Infrared/Terahertz and Low-Frequency Raman Spectroscopy, *Macromolecules*, 2021, **54**(2), 1052–1062.
64 M. Dong, Q. Zhang, X. Xing, W. Chen, Z. She and Z. Luo, Raman spectra and surface changes of microplastics

© 2026 The Author(s). Published by the Royal Society of Chemistry

Open Access Article. Published on 11 May 2026. Downloaded on 6/2/2026 12:52:24 PM. This article is licensed under a Creative Commons Attribution-NonCommercial 3.0 Unported Licence.

weathered under natural environments, *Sci. Total Environ.*, 2020, **739**, 139990.
65 C. Campanale, I. Savino, C. Massarelli and V. F. Uricchio, Fourier Transform Infrared Spectroscopy to Assess the Degree of Alteration of Artificially Aged and Environmentally Weathered Microplastics, *Polymers*, 2023, **15**(4), 911.
66 J. Gubitosa, V. Rizzi, C. Marasciulo, F. Maggi, G. Caprioli, A. M. Mustafa, P. Fini, N. De Vietro, A. M. Aresta and P. Cosma, Realizing Eco-Friendly Water-Resistant Sodium-Alginate-Based Films Blended with a Polyphenolic Aqueous Extract from Grape Pomace Waste for Potential Food Packaging Applications, *Int. J. Mol. Sci.*, 2023, **24**(14), 11462.
67 S. R. Anjana, S. Rawat and S. Goswami, Development of a Biodegradable Ternary Blend of Poly(vinyl alcohol) and Polyhydroxybutyrate Functionalized with Triacetin for Agricultural Mulch Applications, *ACS Omega*, 2024, **9**(28), 30169–30182.
68 J. E. Thomas, L. T. Ou, L. H. Allen, J. C. Vu and D. W. Dickson, Nematode, fungi, and weed control using Telone C35 and colored plastic mulches, *Crop Prot.*, 2009, **28**(4), 338–342.
69 H. Chen, S. Huang, C. Quan, Z. Chen, M. Xu, F. Wei and D. Tang, Effects of different colors of plastic-film mulching on soil temperature, yield, and metabolites in Platostoma palustre, *Sci. Rep.*, 2024, **14**(1), 5110.
70 H. Wu, Q. Liu, W. Sun, Y. Lu, Y. Qi and H. Zhang, Biodegradability of polyethylene mulch film by Bacillus paramycoides, *Chemosphere*, 2023, **311**, 136978.
71 I. Di Mola, V. Ventorino, E. Cozzolino, L. Ottaiano, I. Romano, L. G. Duri, O. Pepe and M. Mori, Biodegradable mulching *vs.* traditional polyethylene film for sustainable solarization: Chemical properties and microbial community response to soil management, *Appl. Soil Ecol.*, 2021, **163**, 103921.
72 H. Somanathan, R. Sathasivam, S. Sivaram, S. Mariappan Kumaresan, M. S. Muthuraman and S. U. Park, An update on polyethylene and biodegradable plastic mulch films and their impact on the environment, *Chemosphere*, 2022, **307**, 135839.
73 G. Rocha Plácido Moore, S. Maria Martelli, C. Gandolfo, P. José do Amaral Sobral and J. Borges Laurindo, Influence of the glycerol concentration on some physical properties of feather keratin films, *Food Hydrocolloids*, 2006, **20**(7), 975–982.
74 C. Gao, E. Pollet and L. Avérous, Properties of glycerol-plasticized alginate films obtained by thermo-mechanical mixing, *Food Hydrocolloids*, 2017, **63**, 414–420.
75 L. Moity, Y. Shi, V. Molinier, W. Dayoub, M. Lemaire and J.-M. Aubry, Hydrotropic Properties of Alkyl and Aryl Glycerol Monoethers, *J. Phys. Chem. B*, 2013, **117**(31), 9262–9272.
76 K. Sheng, X. Dong, Z. Chen, Z. Zhou, Y. Gu and J. Huang, Increasing the surface hydrophobicity of silicone rubber by electron beam irradiation in the presence of a glycerol layer, *Appl. Surf. Sci.*, 2022, **591**, 153097.
77 H. Yu, X. Huang, L. Zhou and Y. Wang, Incorporation of cinnamaldehyde, carvacrol, and eugenol into zein films for active food packaging: enhanced mechanical properties, antimicrobial activity, and controlled release, *J. Food Sci. Technol.*, 2023, **60**(11), 2846–2857.
78 C. Sun, L. Dai, X. He, F. Liu, F. Yuan and Y. Gao, Effect of heat treatment on physical, structural, thermal and morphological characteristics of zein in ethanol-water solution, *Food Hydrocolloids*, 2016, **58**, 11–19.
79 R. Liu and W. Li, High-Thermal-Stability and High-Thermal-Conductivity Ti3C2Tx MXene/Poly(vinyl alcohol) (PVA) Composites, *ACS Omega*, 2018, **3**(3), 2609–2617.
80 P. A. Song, Z. Xu, Y. Lu and Q. Guo, Bioinspired strategy for tuning thermal stability of PVA via hydrogen-bond cross-link, *Compos. Sci. Technol.*, 2015, **118**, 16–22.
81 M. I. Voronova, O. V. Surov, S. S. Guseinov, V. P. Barannikov and A. G. Zakharov, Thermal stability of polyvinyl alcohol/nanocrystalline cellulose composites, *Carbohydr. Polym.*, 2015, **130**, 440–447.
82 C. D. Bucak and M. O. Sahin, Super-flexible, moldable, injectable, self-healing PVA/B/CMC hydrogels synthesis and characterization, as potential water-retaining agent in agriculture, *Polym. Bull.*, 2023, **80**(6), 6591–6608.
83 Z. Yin, J. Cao, Z. Li and D. Qiu, Optimizing the interaction between poly(vinyl alcohol) and sandy soil for enhanced water retention performance, *RSC Adv.*, 2016, **6**(16), 13377–13383.
84 S. Mallakpour and S. Rashidimoghadam, 10 – Poly(vinyl alcohol)/carbon nanotube nanocomposites: Challenges and opportunities, in *Biodegradable and Biocompatible Polymer Composites*, ed. N. G. Shimpi, Woodhead Publishing, 2018, pp. 297–315.
85 M. Liao, Y. Zhao, Y. Pan, J. Pan, Q. Yao, S. Zhang, H. Zhao, Y. Hu, W. Zheng, W. Zhou and X. Dong, A good adhesion and antibacterial double-network composite hydrogel from PVA, sodium alginate and tannic acid by chemical and physical cross-linking for wound dressings, *J. Mater. Sci.*, 2023, **58**(13), 5756–5772.
86 K. Sirivechphongkul, N. Chiarasumran, M. Saisriyoot, A. Thanapimmetha, P. Srinophakun, K. Iamsaard and Y.-T. Lin, Agri-Biodegradable Mulch Films Derived from Lignin in Empty Fruit Bunches, *Catalysts*, 2022, 1150.
87 T. S. Gaaz, A. B. Sulong, M. N. Akhtar, A. A. H. Kadhum, A. B. Mohamad and A. A. Al-Amiery, Properties and Applications of Polyvinyl Alcohol, Halloysite Nanotubes and Their Nanocomposites, *Molecules*, 2015, **20**(12), 22833–22847.
88 F. Abasalizadeh, S. V. Moghaddam, E. Alizadeh, E. akbari, E. Kashani, S. M. B. Fazljou, M. Torbati and A. Akbarzadeh, Alginate-based hydrogels as drug delivery vehicles in cancer treatment and their applications in wound dressing and 3D bioprinting, *J. Biol. Eng.*, 2020, **14**(1), 8.
89 D. Ji, J. M. Park, M. S. Oh, T. L. Nguyen, H. Shin, J. S. Kim, D. Kim, H. S. Park and J. Kim, Superstrong, superstiff, and conductive alginate hydrogels, *Nat. Commun.*, 2022, **13**(1), 3019.
90 P. Kiattijiranon, R. A. Auras and A. Sane, Enhanced Functional Properties for Packaging Applications Using Sodium Alginate/Starch Bilayer and Multilayer Films, *ACS Appl. Polym. Mater.*, 2024, **6**(8), 4642–4650.
91 Y. Li, H. Chengxin, J. Lan, B. Yan, Y. Zhang, L. Shi and R. Ran, Hydrogel-based temperature sensor with water retention, frost resistance and remoldability, *Polymer*, 2020, **186**, 122027.